The Importance of Accurately Measuring the Range Correlation for Range-Oversampling Processing

SEBASTIÁN M. TORRES AND CHRISTOPHER D. CURTIS

Cooperative Institute for Mesoscale Meteorological Studies, University of Oklahoma, and NOAA/OAR/National Severe Storms Laboratory, Norman, Oklahoma

(Manuscript received 13 April 2012, in final form 7 August 2012)

ABSTRACT

A fundamental assumption for the application of range-oversampling techniques is that the correlation of oversampled signals in range is accurately known. In this paper, a theoretical framework is derived to quantify the effects of inaccurate range correlation measurements on the performance of such techniques, which include digital matched filtering and those based on decorrelation (whitening) transformations. It is demonstrated that significant reflectivity biases and increased variance of estimates can occur if the range correlation is not accurately measured. Simulations and real data are used to validate the theoretical results and to illustrate the detrimental effects of mismeasurements. Results from this work underline the need for reliable calibration in the context of range-oversampling processing, and they can be used to establish appropriate accuracy requirements for the measurement of the range correlation on modern weather radars.

1. Introduction

Range-oversampling processing can be used on pulsed Doppler weather radars to increase the signal-to-noise ratio (SNR) through digital matched filtering (Chiuppesi et al. 1980) or to reduce the variance of estimates by decorrelating oversampled data with a matrix transformation followed by incoherent range averaging (Torres and Zrnić 2003a,b). Early studies showed the feasibility of this type of processing using weather data collected with experimental setups and offline signal processing (Ivić et al. 2003; Torres and Ivić 2005). More recently, a real-time implementation was employed on the National Weather Radar Testbed phased-array radar (NWRT PAR) that resulted in faster scan times (by a factor of 2) with no significant loss in data quality (Curtis and Torres 2011). As range-oversampling processing is feasible on modern digital receivers and signal processing architectures, it becomes increasingly important to understand what calibration measurements are necessary and how accurate they need to be for optimal performance. This is the focus of this paper.

The decorrelation transformations used for range-oversampling processing (e.g., digital matched filtering and whitening) depend solely on the normalized range correlation matrix $\mathbf{C}_V$ (Curtis and Torres 2011). This matrix captures the necessary range correlation information for computing appropriate matrix transformations; hence, it is important to measure it accurately. One of the advantages of range-oversampling processing is that the range correlation of oversampled signals can be measured a priori; that is, assuming uniform reflectivity in the radar resolution volume, the range correlation of oversampled signals depends only on radar parameters, namely, the modified pulse (Torres and Zrnić 2003a). The modified pulse is defined as the envelope of the transmitter pulse convolved with the baseband-equivalent receiver impulse response (i.e., the transmitter pulse shape after passing through the receiver filters); thus, it captures both components of the range correlation (Torres and Curtis 2012). In this paper, we show that accurately measuring the range correlation matrix (directly from the data or derived from the modified pulse) is critical for optimal performance of range-oversampling processing.

In principle, the correlation of samples in range can be measured directly from the actual radar data (Ivić et al. 2003), but this makes a systematic mismeasurement analysis less straightforward. Alternatively, the range correlation can be derived from the measured modified pulse. This method is adopted herein for convenience but without the loss of generality. The modified pulse

Corresponding author address: Sebastian Torres, National Weather Center, 120 David L. Boren Blvd., Norman, OK 73072.
E-mail: sebastian.torres@noaa.gov

DOI: 10.1175/JTECH-D-12-00085.1

can be measured in a couple of ways. One way is to simply capture the return from a strong point target (or from multiple ones to check for consistency). If the target is extremely narrow in range extent (e.g., a metal transmission tower), then the measured response will consist of the original transmitted pulse that is reflected off the target and is modified after passing through the receiver filters. This satisfies the definition of the modified pulse and is one way to accurately measure it. The second way to measure the modified pulse is to inject a delayed version of the transmitted pulse directly into the front end of the radar receiver. Note that an additional receiver channel is required if this measurement is to be carried out when the actual pulse is transmitted. However, this method eliminates the need to find a narrow point target, and the signal level can be set appropriately to accurately measure the modified pulse. Although the path through the antenna is not included, it should not have a significant effect on the measurement. An additional consideration when measuring the modified pulse is the receiver sampling rate. A more accurate measurement of the range correlation can be obtained if the pulse is sampled at a rate higher than that used for oversampling processing (normally a multiple of the range-oversampling rate). However, as will be demonstrated later, sampling at the oversampling rate should be sufficient to derive the range correlation matrix needed for range-oversampling processing.

Having established the intimate connection between range-oversampling processing and the range correlation matrix of oversampled signals, and having outlined procedures to measure the latter, it is essential to examine how inaccurate measurements of the range correlation can affect the performance of range-oversampling processing. As will be shown, one of the major effects of a mismeasured range correlation is reflectivity bias. This bias can be on the order of a few decibels (dB), which can lead, for example, to significantly inaccurate quantitative precipitation measurements. Another effect is an overall degradation in performance; that is, the expected increase in SNR or reduction in variance of estimates is not achieved if the range correlation is measured inaccurately. This affects all of the meteorological variables and can, for example, unexpectedly result in higher variance of estimates for whitened data compared to a digital matched filter, even at high signal-to-noise ratios.

This paper is structured as follows. Section 2 introduces a theoretical framework for studying the effects of mismeasurement of the range correlation matrix. In section 3, the theory is validated using simulations that show how different types of mismeasurements affect the reflectivity bias and degrade the performance of range-oversampling processing. Section 4 shows a case from the NWRT PAR that clearly illustrates the reflectivity biases observed when range-oversampling processing relies on an inaccurate measurement of the range correlation. Finally, the results are summarized along with suggestions for applying this work so that the benefits of range-oversampling techniques can be fully realized.

2. Theoretical analysis

In a nutshell, range-oversampling processing entails acquiring time series data at rates L times higher than with conventional sampling and performing incoherent averaging of transformed datasets. The goal of this processing may be to increase the SNR with a digital matched filter (Chiuppesi et al. 1980) or to reduce the variance of meteorological variable estimates (Torres and Zrnić 2003a). Mathematically, the transformation of range-oversampled signals can be expressed as

$$\mathbf{X}_m = \mathbf{W}\mathbf{V}_m, \tag{1}$$

where $\mathbf{V}_m = [\,V(0, m) \quad V(1, m) \quad \cdots \quad V(L-1, m)\,]^{\mathrm{T}}$ is the column vector of L oversampled signals for a given sample time mT_s ($m = 0, 1, \ldots, M-1$, where M is the number of pulses per dwell; T_s is the pulse repetition time). Oversampled time series data are typically spaced by $T_r = \tau/L$ in range time (τ is the transmitter pulse width) and by T_s in sample time. Here, $\mathbf{W}$ is an L-by-L transformation matrix, and $\mathbf{X}_m$ is the vector of L transformed samples with the same structure as $\mathbf{V}_m$. In general, $\mathbf{W}$ can be any L-by-L complex-valued matrix normalized to satisfy the ''power-preserving condition'' given by Torres et al. (2004) as

$$\mathrm{tr}(\mathbf{W}^{*}\mathbf{C}_V\mathbf{W}^{\mathrm{T}}) = L, \tag{2}$$

where ''tr'' is the matrix trace operation, and superscripts T and * denote matrix transposition and complex conjugation, respectively. In the previous equation, $\mathbf{C}_V$ is the normalized range correlation matrix of raw (i.e., nontransformed) oversampled signals defined as $\mathbf{C}_V = S^{-1}E[\mathbf{V}_m^{*}\mathbf{V}_m^{\mathrm{T}}]$, where S is the true signal power and E is the statistical expectation operator. A special case of $\mathbf{W}$ is the whitening transformation given by $\mathbf{W} = \mathbf{H}^{-1}$, where $\mathbf{H}$ is the matrix square root of $\mathbf{C}_V$, that is, $\mathbf{C}_V = \mathbf{H}^{*}\mathbf{H}^{\mathrm{T}}$(Torres and Zrnić 2003a). Other commonly used transformations, such as digital matched filtering and pseudowhitening, are described by Curtis and Torres (2011).

The normalized range correlation matrix of raw samples can be computed in terms of the modified pulse (Torres and Curtis 2012) as

$$\mathbf{C}_V = \|\mathbf{p}\|^{-2}\mathbf{P}^*\mathbf{P}^{\mathrm{T}}, \tag{3}$$

where $\|.\|$ is the vector-norm operator, $\mathbf{p} = [p(0)p(1)\cdots p(N_p-1)]$ is the modified-pulse vector of length N_p sampled at the same range-oversampling rate of T_r^{-1}, and $\mathbf{P}$ is the L-by-$(N_p + L - 1)$ modified-pulse convolution matrix (referred to as the pulse matrix) given by

$$\mathbf{P} = \begin{bmatrix} p(N_p-1) & \cdots & p(0) & 0 & \cdots & 0 \\ 0 & p(N_p-1) & \cdots & p(0) & & 0 \\ & & \ddots & & \ddots & \\ 0 & \cdots & 0 & p(N_p-1) & \cdots & p(0) \end{bmatrix}. \tag{4}$$

It is not difficult to verify that, as required, (3) is a normalized correlation matrix with ones along its main diagonal. Regardless of the nature of $\mathbf{W}$ (e.g., digital matched filter, pseudowhitening, or whitening), the power-preserving condition in (2) means that range-oversampling processing must rely on accurate knowledge of $\mathbf{C}_V$, herein derived from the modified pulse $\mathbf{p}$. As shown next, any mismatches between the true and measured modified pulses will translate into improper normalizations of $\mathbf{W}$, which may lead to unanticipated biases and/or larger-than-expected variance of estimates.

Next, we compute the biases and variances of spectral moment estimates as a function of the range correlation matrix of transformed oversampled signals. Transformed range-oversampled data $\mathbf{X}$ can be used to estimate the spectral moments of weather signals via estimates of the sample-time autocorrelation function at a few small lags (Doviak and Zrnić 1993); that is, from sample-time lag-k autocorrelation estimates of the form

$$\hat{R}_X^{(S)}(k) = \frac{1}{L(M-|k|)}\sum_{l=0}^{L-1}\sum_{m=0}^{M-|k|-1} X^*(l,m)X(l,m+k); \quad \text{for} \quad k = 0, 1 \tag{5}$$

the signal power, mean Doppler velocity, and spectrum width[1] can be derived as

$$\hat{S} = \hat{R}_X^{(S)}(0), \tag{6}$$

$$\hat{v} = -\frac{v_a}{\pi}\arg[\hat{R}_X^{(S)}(1)], \quad \text{and} \tag{7}$$

$$\hat{\sigma}_v = \frac{v_a\sqrt{2}}{\pi}\sqrt{\left|\ln\left[\frac{\hat{R}_X^{(S)}(0)}{|\hat{R}_X^{(S)}(1)|}\right]\right|}, \tag{8}$$

respectively, where the "hats" designate estimates, v_a is the Nyquist velocity, and "arg" denotes the argument of a complex number. In the previous equations, subscript X is used to indicate that autocorrelation estimates are derived from transformed data, and superscript S is used to denote sample-time autocorrelation (as opposed to range-time autocorrelation, which will be denoted with a superscript R). Because the effects of receiver noise are not the focus of this study, a high SNR is assumed for simplicity. Whereas the bias of (6) can be derived directly, the biases of (7) and (8) can only be approximated. Here, we follow the approach by Benham et al. (1972) and use first-order perturbations of the nonlinear functions of $\hat{R}_X^{(S)}$ at different lags, which are valid at high SNR and relatively large M (Zrnić 1977). Thus, it is possible to find the biases of spectral moment estimators as functions of the expected values of autocorrelation estimates. Using the results from Benham et al. (1972) and Zrnić (1977),

$$\mathrm{Bias}(\hat{S}) = E[\hat{R}_X^{(S)}(0)] - R_X^{(S)}(0), \tag{9}$$

$$\mathrm{Bias}(\hat{v}) \approx -\frac{v_a}{\pi}\,\mathrm{Im}\left\{\frac{E[\hat{R}_X^{(S)}(1)]}{R_X^{(S)}(1)}\right\}, \quad \text{and} \tag{10}$$

$$\mathrm{Bias}(\hat{\sigma}_v) \approx \frac{1}{2\pi\sigma_{vn}}\frac{|R_X^{(S)}(1)|}{R_X^{(S)}(0)}\left(\frac{E[\hat{R}_X^{(S)}(0)]}{R_X^{(S)}(0)} - \mathrm{Re}\left\{\frac{E[\hat{R}_X^{(S)}(1)]}{R_X^{(S)}(1)}\right\}\right), \tag{11}$$

[1] Herein, we focus on the classical lag 0–1 spectrum-width estimator; however, the results also apply to other spectrum-width estimators that are based on the ratio of the autocorrelation at two different lags.

where σ_{vn} is the spectrum width normalized by the Nyquist cointerval ($2v_a$); the quantities with no hat represent true values; and "Re" and "Im" stand for real and imaginary parts of a complex number, respectively. The expected values of sample-time autocorrelation estimates in the right-hand side of (9)–(11) can be determined from (5) as

$$E[\hat{R}_X^{(S)}(k)] = \frac{1}{L(M-|k|)} \sum_{l=0}^{L-1} \sum_{m=0}^{M-|k|-1} E[X^*(l,m)X(l,m+k)], \tag{12}$$

where the expected value inside the double summation can be recognized as the two-dimensional autocorrelation function at range-time lag zero and sample-time lag k, $R_X(0,k)$. This two-dimensional function is separable as the product of one-dimensional range- and sample-time autocorrelations, $R_X^{(R)}(0)R_X^{(S)}(k)$. In this separation, the sample-time term includes the true signal power [i.e., $R_X^{(S)}(0) = S$] such that $R_X^{(R)}(0) = 1$. To write (12) in terms of the range correlation matrix of transformed signals $\mathbf{R}_X$, note that the elements along the main diagonal of this matrix are all equal to $R_X^{(R)}(0)$, such that $\mathrm{tr}(\mathbf{R}_X) = LR_X^{(R)}(0)$. Thus, (12) can be written as

$$E[\hat{R}_X^{(S)}(k)] = R_X^{(R)}(0)R_X^{(S)}(k) = \frac{1}{L}\mathrm{tr}(\mathbf{R}_X)R_X^{(S)}(k), \tag{13}$$

where the range correlation matrix of transformed samples is defined as $\mathbf{R}_X = S^{-1}E[\mathbf{X}_m^*\mathbf{X}_m^{\mathrm{T}}]$. Using (1), $\mathbf{R}_X$ can be expressed in terms of the normalized range correlation matrix of raw samples as $\mathbf{R}_X = \mathbf{W}^*\mathbf{C}_V\mathbf{W}^{\mathrm{T}}$. Thus, unbiased sample-time autocorrelation estimates at every lag are obtained if $L^{-1}\mathrm{tr}(\mathbf{W}^*\mathbf{C}_V\mathbf{W}^{\mathrm{T}}) = 1$, which can be recognized as the power-preserving condition in (2). In other words, proper normalization of $\mathbf{W}$ leads to proper normalization of $\mathbf{R}_X$ and to the identity $\mathbf{R}_X = \mathbf{C}_X$, where $\mathbf{C}_X$ is defined as the normalized range correlation matrix of transformed samples with ones along its main diagonal. However, the power-preserving condition can be met only if $\mathbf{C}_V$ is accurately measured.

Next, we look at the effects of inaccurate measurements of the range correlation matrix. The reader should note that range correlation mismeasurements could arise from many different sources, such as contaminated data, improper methodology, or changes in system hardware; however, the analysis that follows is applicable regardless of the source. In general, if the normalized range correlation matrix of raw samples is mismeasured (denoted with a tilde as $\tilde{\mathbf{C}}_V$, where $\tilde{\mathbf{C}}_V \neq \mathbf{C}_V$), then the power-preserving condition may not be met. Consider a transformation $\tilde{\mathbf{W}}$ derived from the *mismeasured* range correlation matrix $\tilde{\mathbf{C}}_V$, such that $\mathrm{tr}(\tilde{\mathbf{W}}^*\tilde{\mathbf{C}}_V\tilde{\mathbf{W}}^{\mathrm{T}}) = L$. Note that the normalization of $\tilde{\mathbf{W}}$ is carried out by incorrectly assuming that the measured range correlation matrix is accurate. However, the *true* range correlation of transformed oversampled signals depends on $\mathbf{C}_V$; thus, the correct power-preserving condition would be $\mathrm{tr}(\tilde{\mathbf{W}}^*\mathbf{C}_V\tilde{\mathbf{W}}^{\mathrm{T}}) = L$ (note that there is no tilde on top of $\mathbf{C}_V$). As a consequence of this mismatch, $\tilde{\mathbf{W}}$ is not guaranteed to be power preserving. In other words, the expected range-time correlation matrix of transformed samples based on measurements, $\tilde{\mathbf{W}}^*\tilde{\mathbf{C}}_V\tilde{\mathbf{W}}^{\mathrm{T}}$, does not match the truth, $\tilde{\mathbf{R}}_X = \tilde{\mathbf{W}}^*\mathbf{C}_V\tilde{\mathbf{W}}^{\mathrm{T}}$. Further, $\tilde{\mathbf{R}}_X$ is not properly normalized since $\tilde{\mathbf{W}}$ was not derived to ensure that $\mathrm{tr}(\tilde{\mathbf{W}}^*\mathbf{C}_V\tilde{\mathbf{W}}^{\mathrm{T}}) = L$. Although unfeasible in practice (only $\tilde{\mathbf{C}}_V$ is known), $\tilde{\mathbf{C}}_X$ could be obtained through a renormalization of $\tilde{\mathbf{R}}_X$ as

$$\tilde{\mathbf{C}}_X = \frac{\mathrm{tr}(\tilde{\mathbf{W}}^*\tilde{\mathbf{C}}_V\tilde{\mathbf{W}}^{\mathrm{T}})}{\mathrm{tr}(\tilde{\mathbf{W}}^*\mathbf{C}_V\tilde{\mathbf{W}}^{\mathrm{T}})}\,\tilde{\mathbf{R}}_X, \tag{14}$$

where it is easy to show that $\mathrm{tr}(\tilde{\mathbf{C}}_X) = L$.

In the following, spectral moment estimates from $\mathbf{W}$ are denoted with a hat, and those derived from $\tilde{\mathbf{W}}$ with a "tilde." For this analysis it is assumed that $\tilde{\mathbf{C}}_V \neq \mathbf{C}_V$ and, as discussed above, $\tilde{\mathbf{R}}_X$ becomes improperly normalized. Using the result from (13) in (9)–(11), the biases of spectral moment estimates obtained from $\tilde{\mathbf{W}}$ are

$$\mathrm{Bias}(\tilde{S}) = S[L^{-1}\mathrm{tr}(\tilde{\mathbf{R}}_X) - 1], \tag{15}$$

$$\mathrm{Bias}(\tilde{v}) \approx -\frac{v_a}{\pi}\mathrm{Im}[L^{-1}\mathrm{tr}(\tilde{\mathbf{R}}_X)], \quad \text{and} \tag{16}$$

$$\mathrm{Bias}(\tilde{\sigma}_v) \approx \frac{1}{2\pi\sigma_{vn}}\frac{|R_X^{(S)}(1)|}{R_X^{(S)}(0)}\{L^{-1}\mathrm{tr}(\tilde{\mathbf{R}}_X) - \mathrm{Re}[L^{-1}\mathrm{tr}(\tilde{\mathbf{R}}_X)]\}. \tag{17}$$

Note that $\mathrm{tr}(\tilde{\mathbf{R}}_X) = L\tilde{R}_X^{(R)}(0)$ is a real number regardless of how $\tilde{\mathbf{W}}$ is derived; thus, (16) and (17) reduce to zero. Consequently, the bias of signal power estimates depends on the range correlation matrix of transformed samples, whereas Doppler velocity and spectrum width estimates remain unbiased for any degree of mismeasurement. Not surprisingly, unbiased signal power estimates are obtained if $\mathrm{tr}(\tilde{\mathbf{R}}_X) = L$, which is true if $\tilde{\mathbf{C}}_V = \mathbf{C}_V$—that is, if there is no mismeasurement of the range correlation.

The variance of spectral moment estimates derived from $\tilde{\mathbf{W}}$ can also be computed directly for signal power and using perturbation analyses for velocity and spectrum width, as done by Zrnić (1977). Expressions for

these in the context of range oversampling are given by Curtis and Torres (2011); at high SNR, they are

$$\mathrm{Var}(\tilde{S}) = \frac{[E(\tilde{S})]^2}{ML^2}\frac{1}{2\sigma_{vn}\pi^{1/2}}\mathrm{tr}(\tilde{\mathbf{C}}_X^2) = \frac{[SL^{-1}\mathrm{tr}(\tilde{\mathbf{R}}_X)]^2}{ML^2 2\sigma_{vn}\pi^{1/2}}\mathrm{tr}(\tilde{\mathbf{C}}_X^2), \quad (18)$$

$$\mathrm{Var}(\tilde{v}) = \frac{v_a^2}{\pi^2(M-1)L^2}\frac{e^{(2\pi\sigma_{vn})^2}-1}{4\sigma_{vn}\pi^{1/2}}\mathrm{tr}(\tilde{\mathbf{C}}_X^2), \quad \text{and} \quad (19)$$

$$\mathrm{Var}(\tilde{\sigma}_v) = \frac{v_a^2 e^{2(2\pi\sigma_{vn})^2}}{4\pi^4\sigma_{vn}^2(M-1)L^2} \times \frac{e^{(2\pi\sigma_{vn})^2}-4e^{(\pi\sigma_{vn})^2}+3}{4\sigma_{vn}\pi^{1/2}}\mathrm{tr}(\tilde{\mathbf{C}}_X^2). \quad (20)$$

Once again, the reader should note that whereas $\tilde{\mathbf{C}}_X$ is properly normalized (by definition), in general, $\tilde{\mathbf{R}}_X$ is not.

The expressions in (15)–(20) show that a range correlation mismeasurement may lead to unexpected variances of estimates since, in general, $\mathrm{tr}(\tilde{\mathbf{C}}_X^2) \neq \mathrm{tr}(\mathbf{C}_X^2)$ but, more importantly, to a biased signal power estimator, which translates into biased radar reflectivities. Using first-order perturbation analysis, the equation that relates reflectivity and signal power can be used to compute an approximation for the bias of reflectivity estimates in decibels (dB); that is, from

$$\tilde{Z} = 10\log_{10}(\gamma\tilde{S})\,[\mathrm{dB}Z], \quad (21)$$

where γ contains the reflectivity calibration constant and all range-dependent terms (Doviak and Zrnić 1993), it can be shown that

$$\mathrm{Bias}(\tilde{Z}) \approx 10\log_{10}\left[1+\frac{\mathrm{Bias}(\tilde{S})}{S}\right] = 10\log_{10}[L^{-1}\mathrm{tr}(\tilde{\mathbf{R}}_X)]\,[\mathrm{dB}], \quad (22)$$

where we used the result in (15).

The change in estimator variance arising from a mismeasured range correlation can be quantified by taking the ratio of variances of estimates derived from $\tilde{\mathbf{W}}$ to those derived from $\mathbf{W}$. Equations (18)–(20) are used for the former, and the same equations can be applied to the latter by substituting all "tilded" matrices with their "nontilded" counterparts. The substitution is immediate and further simplifications can be done by recognizing that $\mathrm{tr}(\mathbf{R}_X) = L$. The variance ratios for the spectral moments are

$$\frac{\mathrm{Var}(\tilde{S})}{\mathrm{Var}(\hat{S})} = \frac{\mathrm{tr}^2(\tilde{\mathbf{R}}_X)\mathrm{tr}(\tilde{\mathbf{C}}_X^2)}{\mathrm{tr}^2(\mathbf{R}_X)\mathrm{tr}(\mathbf{C}_X^2)} = \frac{\mathrm{tr}^2(\tilde{\mathbf{W}}^*\tilde{\mathbf{C}}_V\tilde{\mathbf{W}}^{\mathrm{T}})}{L^2} \times \frac{\mathrm{tr}[(\tilde{\mathbf{W}}^*\mathbf{C}_V\tilde{\mathbf{W}}^{\mathrm{T}})^2]}{\mathrm{tr}[(\mathbf{W}^*\mathbf{C}_V\mathbf{W}^{\mathrm{T}})^2]}, \quad \text{and} \quad (23)$$

$$\frac{\mathrm{Var}(\tilde{v})}{\mathrm{Var}(\hat{v})} = \frac{\mathrm{Var}(\tilde{\sigma}_v)}{\mathrm{Var}(\hat{\sigma}_v)} = \frac{\mathrm{tr}(\tilde{\mathbf{C}}_X^2)}{\mathrm{tr}(\mathbf{C}_X^2)} = \frac{\mathrm{tr}^2(\tilde{\mathbf{W}}^*\tilde{\mathbf{C}}_V\tilde{\mathbf{W}}^{\mathrm{T}})}{\mathrm{tr}^2(\tilde{\mathbf{W}}^*\mathbf{C}_V\tilde{\mathbf{W}}^{\mathrm{T}})} \times \frac{\mathrm{tr}[(\tilde{\mathbf{W}}^*\mathbf{C}_V\tilde{\mathbf{W}}^{\mathrm{T}})^2]}{\mathrm{tr}[(\mathbf{W}^*\mathbf{C}_V\mathbf{W}^{\mathrm{T}})^2]}; \quad (24)$$

these depend on the true and measured range correlation matrices, $\mathbf{C}_V$ and $\tilde{\mathbf{C}}_V$, and the ideal and actual transformation matrices, $\mathbf{W}$ and $\tilde{\mathbf{W}}$.

The polarimetric variables (i.e., differential reflectivity Z_{DR}, differential phase Φ_{DP}, and magnitude of the copolar correlation coefficient ρ_{HV}) can be analyzed analogously. Perturbation formulas for the biases and variances of these estimators (e.g., Melnikov and Zrnić 2004) can be used to show that all polarimetric variables remain unbiased for any degree of mismatch. Without going into the mathematics, this can be intuitively explained by noticing that Z_{DR} and ρ_{HV}, like σ_v, are based on ratios of auto- and cross-correlation estimates, and Φ_{DP}, similarly to v, is based on the argument of a correlation estimate. Thus, any scaling errors arising from range correlation mismeasurements will cancel out in the ratios or become immaterial after taking the argument. Because of these similarities, it can also be shown that the variance ratios for the polarimetric variables are given by (24). In the next section, Eqs. (22)–(24) are validated with simulations and are used to quantify the effects of relying on an inaccurately measured range correlation.

3. Simulations

The theoretical results derived in the previous section are validated with simulations in this section. Range-oversampled weatherlike signals were simulated using the procedure described by Torres and Zrnić (2003a) and the modified pulse of the NWRT PAR (Zrnić et al. 2007) located in Norman, Oklahoma, where the range-oversampling factor was $L = 4$ (as in the NWRT PAR). Simulated range-oversampled signals were processed using the approach described in the previous section to

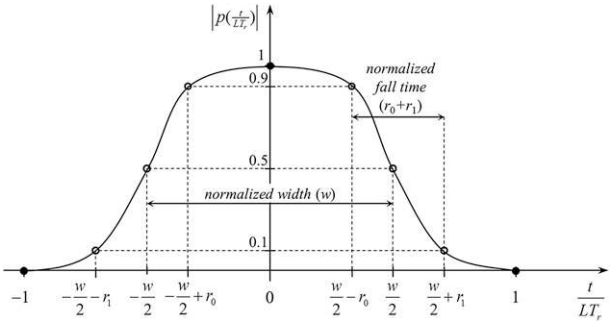

FIG. 1. Magnitude of the modified pulse p, as a function of normalized time t/LT_r, where L is the oversampling factor and T_r is the range sampling period. The amplitude model is based on five control points (represented as "big dots"); two are fixed and three are variable and depend on w, the 3-dB normalized pulse width, r_0 and r_1, where $r_0 + r_1$ is the normalized fall time.

obtain spectral moment estimates for 10 000 realizations of simulated signals with a high SNR of 30 dB and a spectrum width of 2 m s^{-1}, which is typical of many weather phenomena (Fang et al. 2004). Without loss of generality, the Doppler velocity was set to zero because it has no effect on the biases and variances under analysis [cf. (15)–(20)]. A long pulse repetition time (PRT) was used for signal power (reflectivity) estimates, where the number of samples per dwell was $M = 15$ and the Nyquist velocity was $v_a = 7.5$ m s^{-1}. A short PRT was used for mean Doppler velocity and spectrum width estimates, where $M = 40$ and $v_a = 23.7$ m s^{-1}. Range-oversampling processing was carried out using (i) a whitening transformation (whitening-transformation-based estimates are denoted by WTB), (ii) pseudowhitening transformations (PTBs) with sharpening parameter $\alpha = 0.6$ and 0.8 (Torres et al. 2004), and (iii) a digital-matched filter transformation (MFB). As explained next, transformations were derived using mismeasured modified pulses with varying degrees of mismatch in either magnitude or phase.

A model for the modified-pulse shape was chosen so that amplitude and phase mismatches could be systematically varied. The amplitude of the modified pulse was assumed to be symmetric and was obtained by resampling the piecewise-cubic Hermite-polynomial interpolation with control points on the normalized time axis defined at (0,1), ($w/2 - r_0$,0.9), (w/2,0.5), ($w/2 + r_1$,0.1), and (1,0). This type of interpolation is particularly suitable for our purpose because of its shape-preserving properties; that is, it results in no overshoots and less oscillation if the data are not smooth (Fritsch and Carlson 1980). Figure 1 shows a depiction of the amplitude model, where w can be recognized as the 3-dB normalized pulse width and $r_0 + r_1$ as its normalized fall time. The phase of the modified pulse was derived from the phase of the

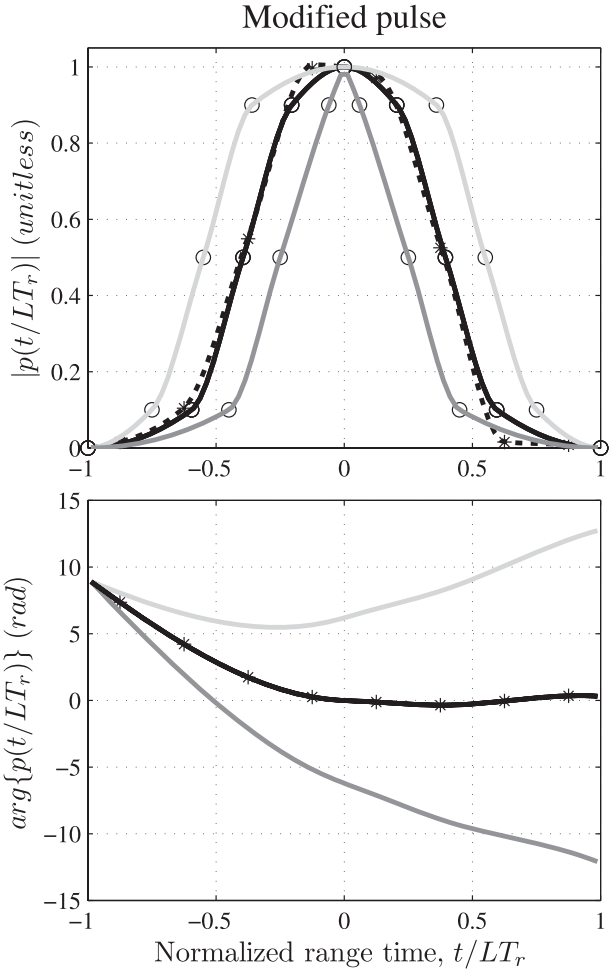

FIG. 2. (top) Magnitude and (bottom) phase of the NWRT PAR modified pulse (dotted line) as a function of normalized range time. Also shown are its best match using the amplitude model with parameters $w = 0.79$, $r_0 = 0.19$, $r_1 = 0.2$, $\phi_0 = 0$, and $\phi_1 = 0$ (solid black line), and the amplitude and phase of the maximally mismatched pulses used in the simulation analysis (solid gray lines). The normalized widths of the maximally mismatched pulses are 0.5 and 1.1, respectively; and the phase slopes are $\pm 90°$ per sample.

NWRT PAR modified pulse (ϕ_{NWRT}) by adding constant and linearly increasing phase terms; that is, $\arg[p(t)] = \phi_{\mathrm{NWRT}} + \phi_0 + \phi_1 t$.

Figure 2 shows the NWRT PAR modified pulse (dotted line) measured using the return from a tower and its best match using our model (solid black line). Also shown in this figure are the amplitudes and phases of the maximally mismatched pulses (solid gray lines) used in the simulation analyses. The model parameters that best match the NWRT PAR pulse are $w = 0.79$, $r_0 = 0.19$, $r_1 = 0.2$, $\phi_0 = 0$, and $\phi_1 = 0$. These are the nominal model parameters used for the simulations; that is, mismatches are obtained by deviating from the nominal parameters, where deviations are denoted by appending Δ to the

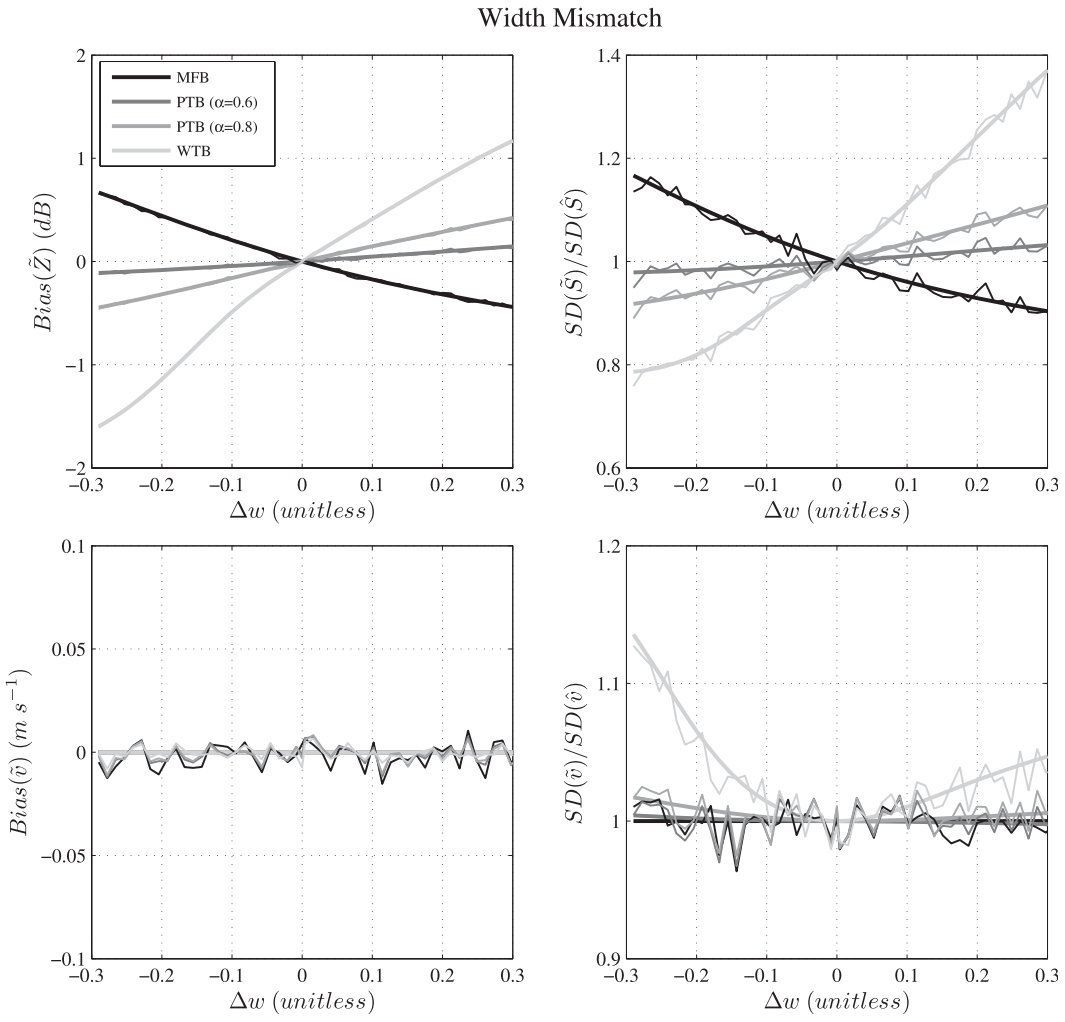

FIG. 3. Theoretical (thick lines) and simulation (thin lines) results for WTB (light gray lines), PTB (medium gray lines), and MFB (black lines) estimates as a function of the normalized width mismatch (Δw). (left) Bias of reflectivity and Doppler velocity estimates using 50 modified pulses with varying degree of mismeasurement. (right) Ratio of standard deviations for signal power and Doppler velocity estimates using the same 50 mismeasured pulses with respect to the true modified pulse.

parameter being changed (e.g., Δw for w). For the maximally mismatched pulses, the normalized widths are $w = 0.5$ and 1.1 (i.e., a Δw of about ± 0.3), respectively, and the slopes of the linear phase shifts are $\phi_1 = \pm 90°$ per sample (i.e., for $N_p = 8$, this results in a maximum shift of $\pm 720°$ that occurs on the last sample).

Figure 3 shows theoretical (thick lines) and simulation (thin lines) results for MFB, PTB, and WTB spectral moment estimates as a function of the normalized width mismatch (Δw). The left plots show the biases of reflectivity [cf. (22)] (top) and mean Doppler velocity [cf. (16)] (bottom). The right plots show the ratio of standard deviations obtained from a mismeasured modified pulse to those obtained from the true modified pulse for signal power and Doppler velocity estimates [cf. (23) and (24)]. A series of 50 modified pulses with normalized widths ranging from 0.5 to 1.1 are used in this analysis. The phases of the modified pulses are set to zero so that the effects of an amplitude mismatch can be independently quantified. Note that $\Delta w = 0$ indicates no mismeasurement; that is, the measured pulse is exactly the true pulse and, as expected, this corresponds to zero reflectivity bias and unit standard deviation ratios. In general, as the degree of mismatch increases, reflectivity biases increase (in absolute value) and range-oversampling processing becomes less effective; that is, the standard deviations of WTB and PTB estimates increase with respect to the expected levels when there are no mismeasurements. The reflectivity bias for MFB estimates increases when the modified-pulse width is measured to be narrower than it

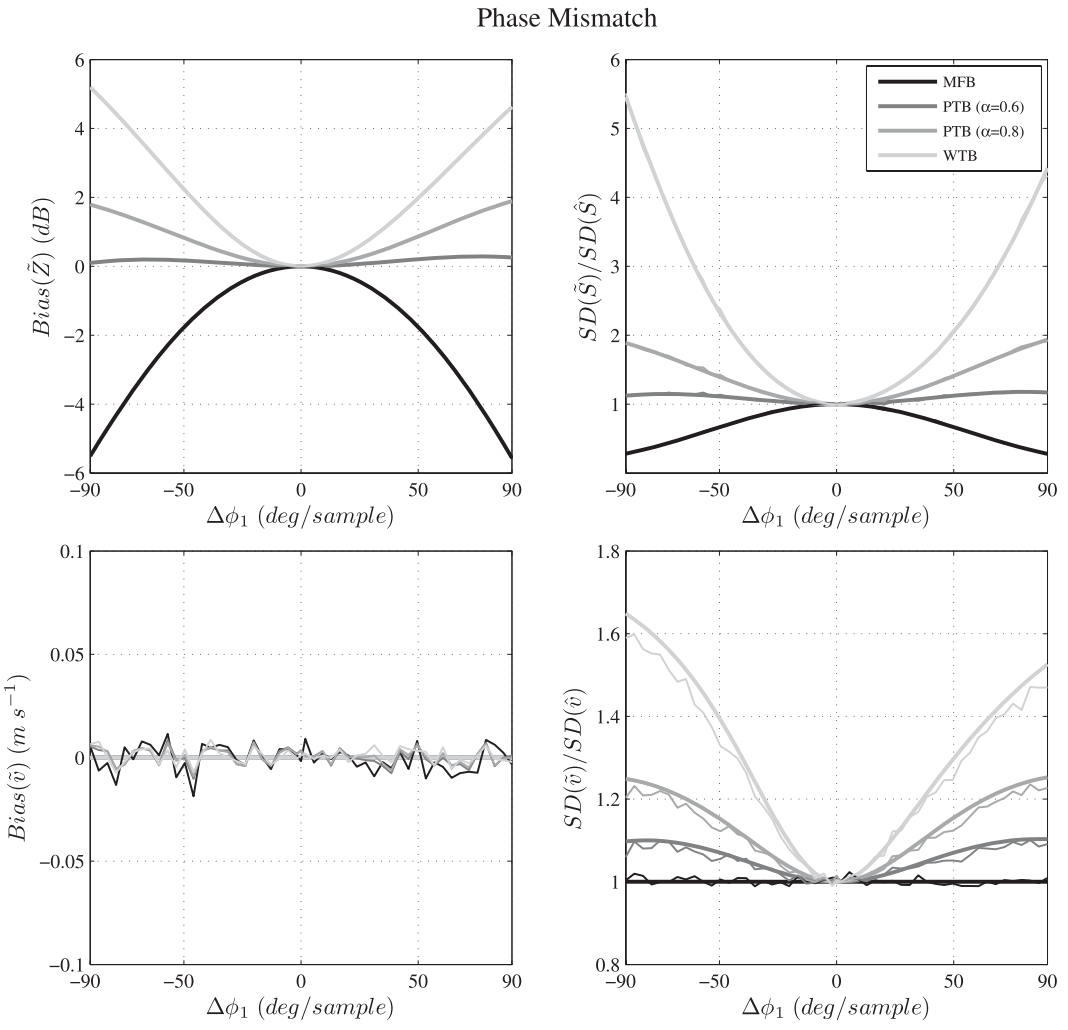

FIG. 4. As in Fig. 3, but as a function of the phase–slope mismatch ($\Delta\phi_1$).

actually is. WTB estimates exhibit the opposite behavior, and PTB estimates fall in between, depending on the degree of pseudowhitening (i.e., $0 < \alpha < 1$, ranging from MFB-like to WTB-like performance). For the range of width mismatches used in this simulation, the maximum absolute reflectivity bias is about 1.5 dB, which occurs for WTB estimates and a measured modified pulse narrower than the true one. The ratios of standard deviations for signal power estimates follow the same trends as the reflectivity biases. It is important to observe that although standard deviation ratios less than one would imply that transformations derived from a mismeasured range correlation matrix are more effective at reducing the variance of estimates, this is not the case for signal power estimates (top-right panel) since these are severely biased (top-left panel). Conversely, the ratios of standard deviations for velocity (and spectrum width) estimates (bottom-right panel) are more meaningful since these estimates are unbiased (bottom-left panel) irrespective of any mismeasurements. It is also worth noting that MFB velocity estimates are almost unaffected by the modified-pulse width mismatch, PTB estimates are minimally affected, and WTB estimates are affected with very modest departures from the ideal behavior (a maximum of about 10% degradation in the standard deviation of velocity estimates).

Figure 4 is the same as Fig. 3, but the results are plotted as a function of the phase–slope mismatch ($\Delta\phi_1$). A series of 50 modified pulses with linear phase shifts ranging from $-90°$ to 90° per sample are used in this analysis. In this case, the amplitudes of the modified pulses are always set to the amplitude of the NWRT PAR modified pulse (Fig. 2), and the phases are perturbed using those of the NWRT PAR modified pulse as a reference; that is, $\Delta\phi_1 = 0$ indicates no mismeasurement (in amplitude or phase), which again corresponds

to zero bias and unit standard deviation ratios. As before, reflectivity estimates become more biased and range-oversampling processing becomes less effective as the degree of mismatch increases. However, whereas the reflectivity bias for MFB estimates becomes more negative (referred to as the ''cold'' radar effect), those of WTB estimates become more positive (''hot'' radar effect). For the range of phase mismatches in this simulation, Doppler velocity estimates are unbiased and the maximum reflectivity bias is about ±5 dB, and positive for WTB estimates and negative for MFB estimates. As expected, the ratio of standard deviations for signal power estimates follows the same trends as the reflectivity bias and, again, standard deviation ratios less than one are not an indication of higher effectiveness at reducing the variance of estimates because of the negative bias of signal power estimates. The ratios of standard deviations for velocity (and spectrum width) estimates exhibit a different behavior. It can be observed that MFB velocity estimates are, like before, almost unaffected by modified-pulse width mismatches. However, WTB estimates are maximally affected with up to 60% degradation from the ideal behavior, and, not surprisingly, the effects on PTB velocity estimates depend on the degree of pseudowhitening.

Similar analyses were conducted for the polarimetric variables, but they are not shown here because the bias and standard deviation ratio plots look nearly identical to those corresponding to mean Doppler velocity. We also conducted simulations varying the other modified-pulse model parameters. Fall-time mismatches (nonzero Δr_0 and Δr_1) lead to performance degradations similar to those observed with pulse width mismatches. However, phase measurement errors in the form of constant biases (nonzero $\Delta\phi_0$) do not affect the performance of any of the range-oversampling techniques. It is important to note that, in all cases, the agreement between theoretical and simulation results is remarkable. In the next section, real data are used to illustrate the impact of these results.

4. Effects on data

The effects of mismeasurement of the modified pulse can be shown using collected time series data. For this comparison, data from 11 February 2009 were acquired using a long PRT T_s = 3104 ms (v_a = 7.5 m s^{-1}) and M = 15 samples per dwell for reflectivity, and a short PRT T_s = 984 ms (v_a = 23.7 m s^{-1}) and M = 40 samples per dwell for mean Doppler velocity and spectrum width. Long- and short-PRT datasets were processed with both an accurately measured modified pulse and a ''mismeasured'' modified pulse. To obtain the mismeasured modified pulse, the phase of the NWRT PAR modified pulse was altered as described in section 3 with $\Delta\phi_1 = 90°$ per sample. Figures 5 and 6 show plan position indicator (PPI) displays of reflectivity and Doppler velocity fields at ~0159 UTC. In each of these figures, the three left panels show data processed with the accurately measured modified pulse, and the three right panels show data processed with the ''mismeasured'' modified pulse. The top two panels show the results utilizing a digital-matched filter, the middle two panels show the results for pseudowhitening with α = 0.6, and the bottom two panels show the results for whitening. This allows us to see the differing effects of mismeasurement on the three types of processing.

The digital-matched filtered data with the accurately measured modified pulse is used as the baseline for comparisons (top-left panel). Since the pseudowhitening and whitening transformations should be power preserving, the reflectivity levels shown in the middle and bottom right panels of Fig. 5 should match but should also look smoother because of the variance reduction obtained from these transformations. We do see that the data become progressively smoother when moving from digital-matched filtering to pseudowhitening to whitening, and the reflectivity levels also seem to match reasonably well. To quantify the effects of both modified pulses and all processing transformations, reflectivity differences between the datasets were utilized. The datasets were compared to the baseline digital-matched filtered dataset with an accurately measured modified pulse, and an SNR threshold of 20 dB was used to ensure that the comparisons were made using strong signals. Because of some large outliers in the reflectivity differences, the median was used to measure the central tendency. In the whitening case with an accurately measured pulse (bottom-left panel), the median difference in reflectivity values is 0.05 dB, which shows that the reflectivity levels are basically the same. For pseudowhitening, the median reflectivity difference is 0 dB.

For the ''mismeasured'' modified pulse, the differences in reflectivity are striking. The digital-matched filtered data (top-right panel) looks significantly ''colder'' than those from the accurately measured case. The median difference in reflectivity is −5.36 dB, which is close to the theoretically predicted value of −5.20 dB (see Fig. 4). As expected, the whitened data (bottom-right panel) look ''hotter'' than the accurately measured case. The median reflectivity difference is 4.43 dB, which also matches well compared to the theoretically predicted bias of 4.54 dB. The pseudowhitened data (middle-right panel) exhibit a smaller bias of 0.24 dB, nearly matching the theoretical value of 0.27 dB. A secondary effect of these biases can be seen in the different amounts of censoring between the

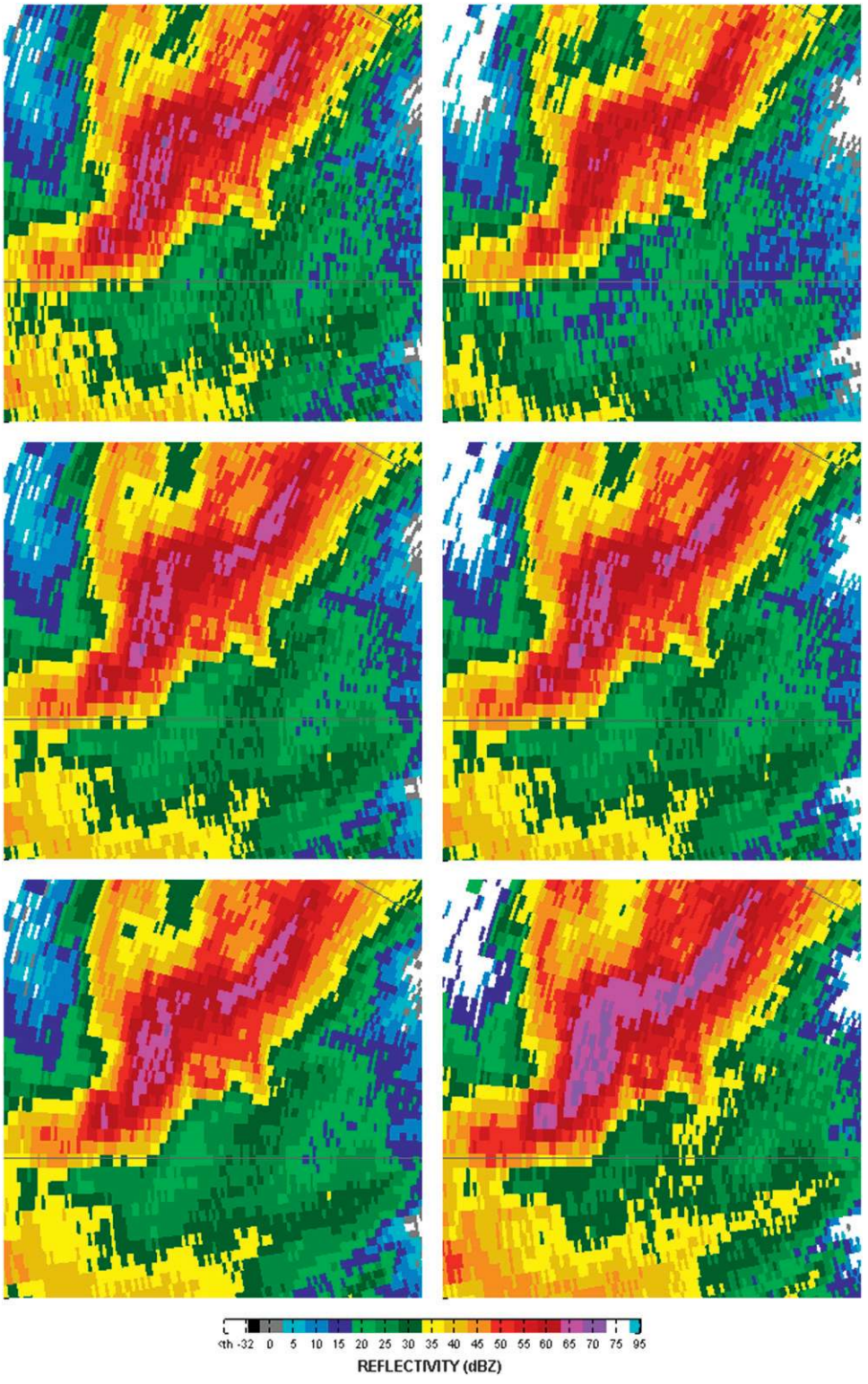

FIG. 5. PPI displays (30 km × 30 km) of reflectivity fields using (left) an accurately measured modified pulse and (right) a mismeasured modified pulse. (top) Digital-matched filter processing, (middle) pseudowhitening processing with $\alpha = 0.6$, and (bottom) whitening processing were utilized to show the differing effects of mismeasurement.

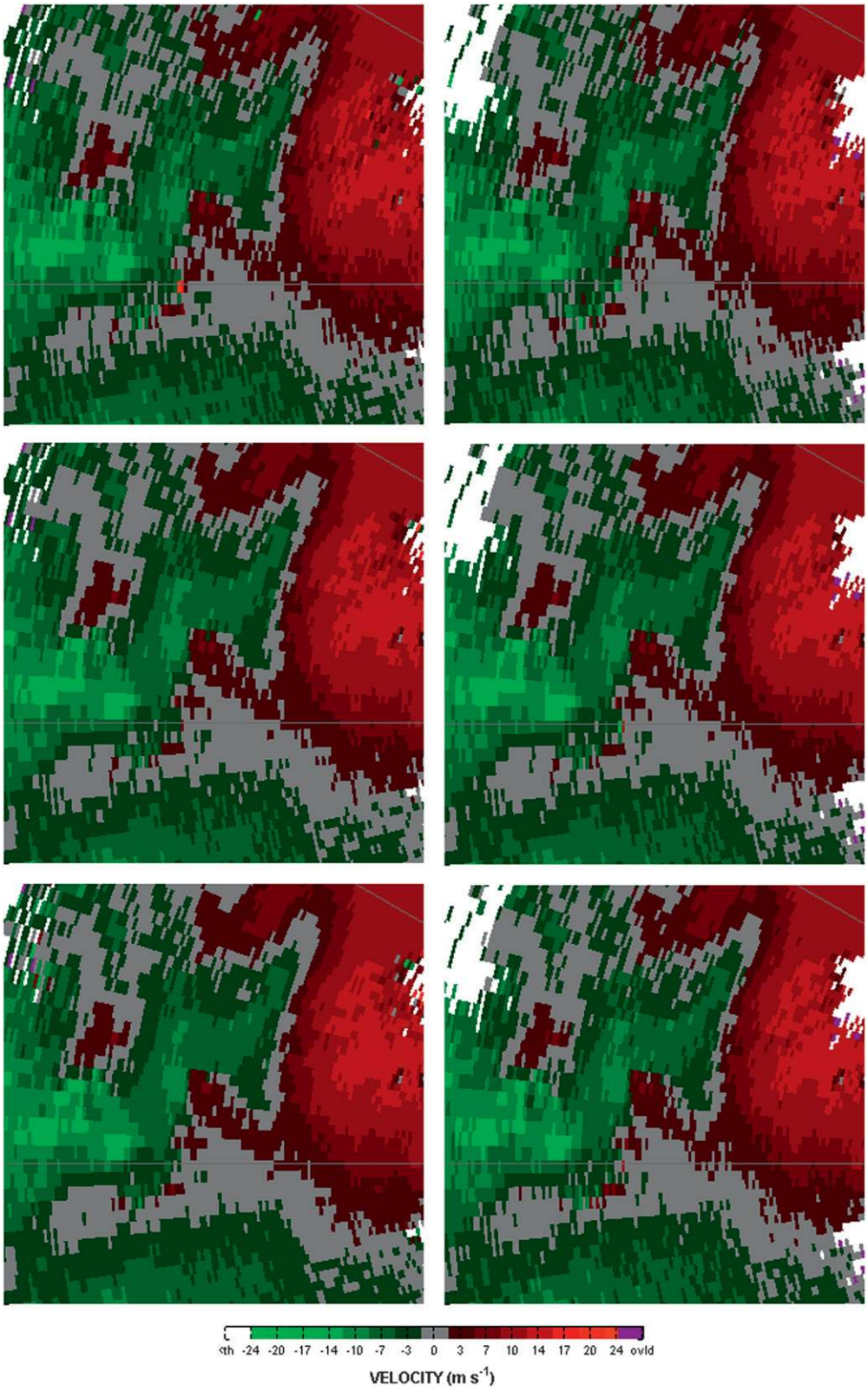

FIG. 6. As in Fig. 5, but for mean Doppler velocity fields.

left and right panels of Figs. 5 and 6; this censoring is based on the MFB signal power for all transformations, and thus all the ''mismeasured'' fields are affected in the same way. Although it is more difficult to see the effects of increased standard deviation, the whitened data using the mismeasured pulse do look less smooth than the whitened data using the accurately measured pulse. Even though this is an extreme example, substantial reflectivity biases can occur for smaller measurement errors, a fact that reinforces the case for accurate measurement of the range correlation. For instance, after changing a trigger amplifier on the NWRT PAR and before updating the range correlation measurement to reflect this change, we observed reflectivity biases of −3.16 and 3.46 dB when using a digital-matched filter and a whitening transformation, respectively.

As predicted by the theory, the biases in the mean Doppler velocity data are close to zero. As with the reflectivity, the velocity data become progressively smoother when moving from digital-matched filtering to pseudowhitening to whitening. Although fields of spectrum width are not included, the results are similar to those in Fig. 6. In a dual-polarimetric radar, we would also expect to see no biases in differential reflectivity, differential phase, and magnitude of the copolar correlation coefficient.

5. Conclusions

Range-oversampling techniques rely on accurate knowledge of the range correlation to derive time series data transformations that can improve the signal-to-noise ratio (e.g., digital matched filter) or reduce the variance of meteorological data estimates (e.g., whitening). The range correlation can be measured directly from the data or derived from measurements of the modified pulse. In this paper, we explored the effects of having a mismeasured range correlation on the performance of range-oversampling techniques.

A theoretical framework was developed to quantify the effects of mismeasurement in terms of the statistical performance of range-oversampling techniques based on a digital matched filter, whitening, and pseudowhitening transformations. Whereas reflectivity estimates can be severely biased depending on the degree of mismeasurement, all other meteorological variables were shown to remain unbiased under any mismeasurement conditions. However, range-correlation mismeasurements cause the standard deviations of all estimates to increase, except for reflectivity, which may have lower standard deviations because of the negative biases. Simulations based on a parametric model of the modified pulse were used to validate the theoretical results. Examples of both amplitude and phase mismatches were studied and shown to agree with the theoretical predictions. A real-data case was used to illustrate the performance degradation that can occur when there is a severe mismeasurement of the modified pulse; this also agreed well with simulations and theoretical results.

As range-oversampling techniques become more widely used, it is important to understand how a mismeasurement of the range correlation can affect their performance. The framework provided in this paper can be used to translate radar data quality requirements into concrete specifications for the accuracy of range correlation measurements on modern operational weather radars, and thus ensure that the benefits of range-oversampling techniques are fully realized.

Acknowledgments. The authors thank Dusan Zrnić, Igor Ivić, and three anonymous reviewers for providing comments to improve the manuscript. Funding was provided by NOAA/Office of Oceanic and Atmospheric Research under NOAA–University of Oklahoma Cooperative Agreement NA11OAR4320072, U.S. Department of Commerce.

REFERENCES

Benham, F. G., H. L. Groginsky, A. S. Soltes, and G. Works, 1972: Pulse pair estimation of Doppler spectrum parameters. Air Force Cambridge Research Laboratories Rep. AFCRL-72-0222, Raytheon Contract F19628-71-C-0126, 148 pp.

Chiuppesi, F., G. Galati, and P. Lombardi, 1980: Optimisation of rejection filters. *IEE Proc.,* **127F,** 354–360.

Curtis, C. D., and S. M. Torres, 2011: Adaptive range oversampling to achieve faster scanning on the National Weather Radar Testbed phased-array radar. *J. Atmos. Oceanic Technol.,* **28,** 1581–1597.

Doviak, R., and D. Zrnić, 1993: *Doppler Radar and Weather Observations*. 2nd ed. Academic Press, Inc., 562 pp.

Fang, M., R. Doviak, and V. Melnikov, 2004: Spectrum width measured by WSR-88D: Error sources and statistics of various weather phenomena. *J. Atmos. Oceanic Technol.,* **21,** 888–904.

Fritsch, F., and R. Carlson, 1980: Monotone piecewise cubic interpolation. *SIAM J. Numer. Anal.,* **17,** 238–246.

Ivić, I. R., D. S. Zrnić, and S. M. Torres, 2003: Whitening in range to improve weather radar spectral moment estimates. Part II: Experimental evaluation. *J. Atmos. Oceanic Technol.,* **20,** 1449–1459.

Melnikov, V., and D. Zrnić, 2004: Simultaneous transmission mode for the polarimetric WSR-88D: Statistical biases and standard deviations of polarimetric variables. NOAA/NSSL Rep., 84 pp.

Torres, S. M., and D. S. Zrnić, 2003a: Whitening in range to improve weather radar spectral moment estimates. Part I: Formulation and simulation. *J. Atmos. Oceanic Technol.,* **20,** 1433–1448.

——, and ——, 2003b: Whitening of signals in range to improve estimates of polarimetric variables. *J. Atmos. Oceanic Technol.,* **20,** 1776–1789.

——, and I. R. Ivić, 2005: Demonstration of range oversampling techniques on the WSR-88D. Preprints, *32nd Conf. on Radar Meteorology,* Albuquerque, NM, Amer. Meteor. Soc., 4R.5. [Available online at https://ams.confex.com/ams/32Rad11Meso/techprogram/paper_96151.htm.]

——, and C. D. Curtis, 2012: The impact of signal processing on the range-weighting function for weather radars. *J. Atmos. Oceanic Technol.,* **29,** 796–806.

——, ——, and J. R. Cruz, 2004: Pseudowhitening of weather radar signals to improve spectral moment and polarimetric variable estimates at low signal-to-noise ratios. *IEEE Trans. Geosci. Remote Sens.,* **42,** 941–949.

Zrnić, D. S., 1977: Spectral moment estimates from correlated pulse pairs. *IEEE Trans. Aerosp. Electron. Syst.,* **13,** 344–345.

——, and Coauthors, 2007: Agile-beam phased array radar for weather observations. *Bull. Amer. Meteor. Soc.,* **88,** 1753–1766.